

RESEARCH

Open Access



Distinct and additive effects of visual and vibratory feedback for motor rehabilitation: an EEG study in healthy subjects

Ahmed Adham^{1,2,4*}, Hugo Bessaguet^{1,3}, Lucas Struber⁴, Diana Rimaud¹, Etienne Ojardias^{1,2} and Pascal Giraux^{1,2}

Abstract

Introduction The use of visual and proprioceptive feedback is a key property of motor rehabilitation techniques. This feedback can be used alone, for example, for vision in mirror or video therapy, for proprioception in focal tendon vibration therapy, or in combination, for example, in robot-assisted training. This Electroencephalographic (EEG) study in healthy subjects explored the distinct neurophysiological impact of adding visual (video therapy), proprioceptive (focal tendinous vibration), or combined feedback (video therapy and focal tendinous vibration) to a motor imagery task.

Methods Sixteen healthy volunteers performed 20 mental imagery (MI) tasks involving right wrist extension and flexion under four conditions: MI alone (IA), MI + video feedback observation (IO), MI + vibratory feedback (IV), and MI + observation + vibratory feedback (IOV). Brain activity was monitored with EEG, and time-frequency neurophysiological markers of movement were computed. The emotions of the patients were also measured during the task.

Results In the alpha band, we observed bilateral ERD in the visual feedback conditions (IO, IOV). In the beta band, the ERD was bilateral in the IA, IV and IOV but more lateralized in the IV and IOV. After movement, we observed strong ERS in the IO and IOV but not in the IA or IV. Embodiment was stronger in conditions with vibratory feedback ($\text{IOV} > \text{IV} > \text{IA}$ and IO)

Conclusion Conditions with visual feedback (IO, IOV) recruit the mirror neurons system (alpha ERD) and provide more accurate feedback of the task than IA and IV, which triggers motor validation pathways (beta rebound analysis). Vibratory feedback enhances the recruitment of the left sensorimotor areas, with a synergistic effect in the IOV (beta ERD analysis), thus maximizing embodiment. Visual and vibratory feedback recruits the sensorimotor cortex during motor imagery in different ways and can be combined to maximize the benefits of both techniques

Trial registration <https://clinicaltrials.gov/study/NCT04449328>.

Keywords Motor imagery, Video therapy, Focal vibration therapy, EEG, Rehabilitation

*Correspondence:
Ahmed Adham
ahmed.adham@chu-st-etienne.fr

Full list of author information is available at the end of the article



© The Author(s) 2024, corrected publication 2025. **Open Access** This article is licensed under a Creative Commons Attribution-NonCommercial-NoDerivatives 4.0 International License, which permits any non-commercial use, sharing, distribution and reproduction in any medium or format, as long as you give appropriate credit to the original author(s) and the source, provide a link to the Creative Commons licence, and indicate if you modified the licensed material. You do not have permission under this licence to share adapted material derived from this article or parts of it. The images or other third party material in this article are included in the article's Creative Commons licence, unless indicated otherwise in a credit line to the material. If material is not included in the article's Creative Commons licence and your intended use is not permitted by statutory regulation or exceeds the permitted use, you will need to obtain permission directly from the copyright holder. To view a copy of this licence, visit <http://creativecommons.org/licenses/by-nc-nd/4.0/>.

Introduction

Mental imagery (MI) is defined as the voluntary activation of a mental representation of a movement without the movement actually being performed [1]. It can be kinesthetic (the subject feels that he or she is performing a movement) or visual (the subject visualizes himself/herself in the first or third person performing a movement) [2]. For healthy subjects, MI allows the subjects to stimulate and maintain the cortical networks involved in motor function, particularly the motor, premotor, prefrontal and parietal regions [3]. MI has also been shown effective in addition to conventional rehabilitation in poststroke rehabilitation, with improvements in motor function of the upper limb, walking speed and functional independence [4, 5]. From a neurophysiological perspective, MI increases functional connectivity between motor and premotor regions [6], corticospinal excitability [7] and induces structural connectivity reorganization [8].

Current rehabilitation techniques propose enriching MI with various feedback, notably visual (visual feedback therapies: mirror therapy, virtual reality therapy) and kinesthetic feedback (i.e., tendinous vibration therapies), to facilitate motor imagery and to provide proprioceptive and/or visual feedback on a correctly performed action.

Visual feedback therapies (VfT) are diverse. Historically, mirror therapy (MT) was the first rehabilitation technique to offer patients subjective visual feedback of correct movement performed by a paretic limb [9, 10]. However, during the last decade, video observational therapy (VOT) has emerged as an alternative to mirror therapy. In this therapy, the subject observes on a screen a projection of the paretic limb performing the action. This projection is made using a prerecorded video of the healthy limb performing the action flipped on the horizontal axis (mirror image) and displayed on a screen (Fig. 1). The VOT provides the subject with the subjective visual illusion of a correctly performed movement



Fig. 1 Video observational feedback therapy (IVS-3TM - Dessaintey)

without requiring the use of a healthy limb. The benefits of VfT have been widely demonstrated not only in motor rehabilitation for central nervous system impairments, such as stroke [11, 12], but also in peripheral nervous system rehabilitation, such as brachial plexus palsy [13].

Vibratory feedback therapy consists of exciting muscle spindles by means of vibratory stimulation. These vibrations can be applied to the whole body or in a focal manner (focal vibration, FV). Vibratory stimulation devices are generally applied to tendons or related muscles (e.g., *biceps brachialis* and *extensor radialis longus carpi*). In stroke rehabilitation but also in other neurological disease rehabilitation (i.e., multiple sclerosis, cerebral palsy), FV has shown benefits for balance, motor function and spasticity [14, 15].

Visual and proprioceptive feedback, whether provided by video therapy devices, focal vibration, or other devices, is at the heart of modern rehabilitation techniques (i.e., robotic therapy seeks to provide somato-sensori feedback to the subject, along with a visual feedback of the moving arm). We know that visual feedback induces a rebalance of interhemispheric inhibition in healthy subjects [16] and stroke patients [17]. Similarly, we know that FV facilitates the recruitment of the sensory-motor regions of the subject [18, 19], with an improvement in the efficiency of the sensorimotor network [20]. However, the way each of these feedbacks might act precisely on the sensorimotor cortex remains imperfectly understood. Additionally, the synergy between visual and proprioceptive feedback remains to be explored. The addition of a vibration device to mirror therapy or virtual reality promotes the illusion of subjectivity of movements [21] as well as the perceived motor illusion of the subjects [22]. In electroencephalography (EEG), Le Franc et al. reported increased recruitment in sensory-motor regions under combined FV and VOT conditions compared to imaging conditions alone [23]. Interestingly, proprioceptive afferences alone [24] but also coupled to visual feedback [25] also enhance classification performances in motor imagery tasks in Brain Computer Interfaces training.

However, despite those results, a major challenge remains in to create a standardized and easily reproducible neurophysiological experiment in healthy subjects, that can be later extended to stroke patients, to specifically explore the integration of each type of feedback with the aim to personalize the rehabilitation therapy [26]. The aim of the study is to get a better understanding of the integration of visual, somato-sensory, and coupled feedback, along with a point of comparison for subsequent data for stroke patients.

To build this model, we recorded the EEG activity of healthy subjects performing motor imagery tasks of the right wrist under experimental conditions with visual, proprioceptive, or double feedback. For visual feedback,

we chose the VOT since it enabled us to study the specific effect of visual feedback without being disturbed by the cortical activities inherent to the production of the movement of the other limb in the MT. For proprioceptive feedback, the FV allowed us to study the specific effects of proprioceptive feedback. Four experimental conditions were tested: [1] imagery alone—IA; [2] imagery with visual feedback observation—IO; [3] imagery with vibratory feedback—IV; and [4] imagery with visual and vibratory feedback—IOV; with the study of EEG alpha and beta desynchronization during the task and beta rebound after the task.

Materials and methods

Participants

We recruited right-handed healthy volunteers. We excluded subjects who presented with neurological, epileptic, or psychiatric illness and subjects who were receiving neuromodulatory treatments or neuromodulatory drugs. Participants signed a consent form prior to participating in the study. Participants underwent the Edinburgh Handedness Inventory test of laterality, and we also tested their visual imagery performance with the Movement Imagery Questionnaire-Revised (MIQ-RS) questionnaire [27].

The inclusions were conducted between January and April 2023. The STROBE guidelines were used to report our study. The study was registered at NCT (NCT04449328). The study was conducted in accordance with the Declaration of Helsinki and was approved by the ethics committee. Comité de protection des personnes Sud Ouest et Outre Mer IV" (04/12/2019. N°: CPP2019-11-084a / 2019-A01673-54 / 19.09.12.44858 with amendment N°: 19.01592.201984-MS03 allowing EEG data collection for healthy subjects).

Material

Visual feedback was provided using a VOT device (IVS-3™-Dessintey™). It consists of a large screen precisely placed between the subject's eye and his trained hand. The device is equipped with a camera behind its screen that records a hand movement as if it were in first-person view. When a recorded video is displayed on the screen, it results in the illusion of subjective movement. Medical foam was placed under the wrist to sur-elevate the hand and make movements more comfortable. This device can easily provide congruent feedback with the visual axis, thus maximizing the subjective illusion (Fig. 2A).

Vibratory feedback was provided using the Vibrasens device (VB 115, Techno Concept™). The Vibrasens is composed of a generator with adjustable vibration frequency, as well as a vibrator with an interchangeable tip, which can be placed on the wrist of the subjects (Fig. 2B). The device was placed on the tendon of the *extensor radialis longus carpi*, with the adapted tip.

EEG data were recorded with a 32-channel ENOBIO™ device placed on the head of the subjects with Ag/AgCl electrodes. The data were sampled at 500 Hz, and the impedance was maintained below 5 kHz. The protocol displayed on the IVS panel was designed with OpenSesame software [28]. An OpenSesame Time To Live (TTL) trigger was sent on the EEG recording at the beginning of each experimental condition for accurate synchronization of the visual cues in further analysis.

Experimental device

During the experiment, the subjects were comfortably installed in a standardized position on a chair in front of a height-adjustable table on which they trained on VOT.

Before the beginning of the session and during the entire duration of the experiment, the subject's right hand was positioned behind the screen of the VOT device. Then, the vibration device was applied to the subject's right *extensor radialis longus carpi* tendon. For each

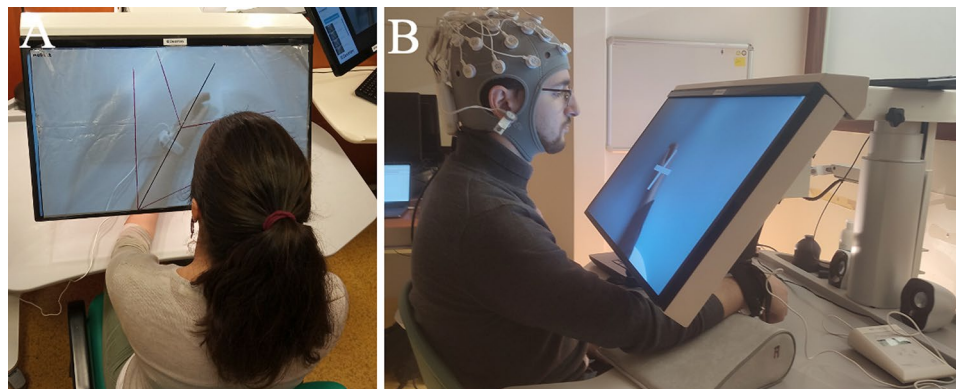


Fig. 2 (A) Standardization of movement amplitude with a transparent layer. (B) Experimental setup, with a video-feedback therapy device, an EEG device and a vibratory feedback device

subject, we searched the vibration frequency that maximized the subject's self-declared kinesthetic illusion in a 70 to 100 Hz vibratory range [29]. The vibration amplitude was set to 1 mm [18]. We then recorded the following with VOT device:

1. A video of the subject's hand performing a wrist extension and returning to a neutral position. The video was then manually extracted from the VOT device, shortened, and resampled for the whole movement to last exactly three seconds, with two seconds of pause before and after. The movement displayed and performed by the subjects consisted of a slow extension of the wrist and fingers (two seconds) immediately followed by quick flexion (one second). At rest, the wrist was in a neutral position on the axis of the arm and was completely relaxed. The amplitude of the movement and position of the hand on the screen were standardized due to the use of a transparent layer with angle markers placed on the screen during the recording of the video and removed afterward (Fig. 2B). The timing of the movement was as follows: two seconds of presentation of the arm with a white cross, 3 s of task (2 s of hand opening and one second of return to rest), and then 2 s of rest with the return of the cross, added to a randomized time of 500 to 1000 milliseconds. This video was used for the imagery + observation (IO) and imagery + observation + vibration conditions (IOV).

2. In the six-second video of the panel of the VOT device, we added the same cross as in the first video. This video was used for the imagery alone (IA) and imagery + vibration conditions (IV). We deliberately did not show a video of the subject's immobile hand to prevent incongruent feedback interference (feeling of a hand movement while watching an immobile hand).

Each session was divided into four subsessions, separated by a one-minute pause, and proposed in a randomized order to each subject. In each subsession, the subject performed a motor imagery task of right wrist dorsiflexion twenty times and returned to rest (Fig. 3). The subsessions differed in the type of feedback offered in addition to the motor imagery task. In the IA subsession, the subject had to imagine only the MI task without visual or vibratory feedback. In the IO subsession, the subject performed the MI task while observing the movement performed on the VOT device. In the IV task, the subject had to perform MI with congruent vibratory feedback during wrist extension but without visual feedback. The vibratory feedback was manually synchronized with the action by the same operator in all the studies. In the IOV subsession, the subject had to perform MI, with vibratory feedback and visual feedback.

After each group of 20 movements for each condition, a one-minute break was observed. During this time, the subjects were asked to rate the intensity of their subjective imagery perception on a Likert scale ranging from 1 to 10. They were also asked to mimic the angle of

| Duration: | 2 seconds | 2 seconds | 1 second | 2 seconds |
|-----------------------------------|---|----------------------------------|--|-----------|
| Task: | Rest | Motor imagery of wrist extension | Motor imagery of wrist coming back to position | Rest |
| Visual feedback in: IA, IV | | | | |
| Visual feedback in: IV, IOV | | | | |
| Vibratory feedback in: IV, IOV | No | Yes | Yes | No |
| Vibratory feedback in: IA, IO | No <i>(The vibratory device remains on the subject's hand but is not working)</i> | | | |

Fig. 3 Experimental paradigm for the imagery alone (IA), imagery + observation (IO), imagery + vibration (IV), and imagery + observation + vibration (IOV) conditions

movement felt with their right hand. The angle was measured with an electronic goniometer.

Data analysis

EEG

After filtering (0.5–70 Hz bandpass filter, 50 Hz notch filter), the data were segmented into 7-second epochs (2 s before the onset of movement and 2 s after the end of movement). The epochs containing a peak-to-peak voltage above 100 mV were considered too noisy and rejected. Then, a visual inspection of the data was conducted with rejection of the remaining noisy epochs, and bad channels were interpolated. Approximately 80% of the data in our study were considered valid. Ocular artifacts were removed with independent component analysis (ICA). This whole process was conducted using the MATLAB EEGLab Toolbox (UC San Diego, USA) [30]. The data were referenced to infinite sources using the REST algorithm [31]. After this preprocessing, for each epoch and each EEG channel, time-frequency maps were generated. We implemented time-frequency analysis by convolving the signal with a set of complex Morlet wavelets, defined as complex sine waves tapered by a Gaussian distribution. The frequencies of the wavelets ranged from 2 Hz to 40 Hz in 80 linearly spaced steps. The full width at half maximum (FWHM) ranged from 1000 to 200 ms [32, 33]. To avoid border effect artifacts during wavelet analysis, we removed 500 ms on each side of the epochs after wavelet convolution.

For each electrode, event-related desynchronization (ERD) and event-related synchronization (ERS) magnitudes were then expressed as percentages of the power in the defined time and frequency window relative to the power measured during the corresponding baseline [34] and were expressed as percent changes. The baseline was chosen between 1500 ms and 500 ms before the onset of the movement. We analyzed [1] alpha band power (8–12 Hz) during the task (2500–4500 ms) to obtain the alpha component of the mu motor rhythm, [2] beta band power (12–25 Hz) during the task (2500–4500 ms) to obtain the beta component of the mu motor rhythm, and [3] beta band power after the task (5000–6000 ms) to obtain the postmovement beta rebound power. The average of all the time-frequency maps for each condition and electrode was computed.

Statistical comparison

EEG data

For statistical analysis, we evaluated the modulations of alpha, beta ERD and beta ERS intensity values for each motor imagery task in two regions of interest, the C3 and C4 electrodes, which represent the activity over the left and right sensory-motor cortex, respectively. This allowed us to explore the effects of the different types of

feedback. Statistical analysis over time-frequency regions of interest was conducted using a Friedman test to assess whether the means of illusion intensities differed significantly across the feedback conditions due to nonnormality of the data. Subsequently, to determine which pairs of conditions exhibited significant differences, post hoc tests were performed with a Wilcoxon signed-rank test with a significance threshold of $p < 0.05$.

To improve statistical relevancy, we also performed time-frequency mapping on C3, C4, CP5, CP6, and occipital region electrodes (mean of Oz, O1 and O2 maps) using permutation testing with 10,000 permutations under the null hypothesis, with a significance threshold of $p < 0.05$ for each test, followed by cluster-based correction to identify contiguous regions exhibiting significant differences [35]. The results of this permutation test, along with the time-frequency maps, are shown in the Supplementary Materials.

Kinesthetic illusion data

For kinesthetic illusion comparison between conditions, the statistical analysis was conducted at first with a Friedman test, to assess whether the means of illusion intensities declared by the subjects significantly differed across the four feedback conditions. If the Friedman test was positive ($p < 0.05$), a Wilcoxon signed-rank post hoc tests was performed to determine which pairs of conditions exhibited significant differences, with a significance threshold of $p < 0.05$ for each pairwise comparison.

Results

Participants

Sixteen healthy volunteers (age: 47.1 years +/- 14.9, with 9 females and 7 males) were recruited for the study from the University of Saint-Etienne. Fifteen subjects were right-handed, and 1 subject was left-handed.

Time-frequency analysis during motor imagery

Alpha band desynchronization

In the alpha band, the time course analysis of the signal over the C3 electrode (Fig. 4A) revealed quick desynchronization in the IA condition (approximately one second) rather than maintained desynchronization during the other three conditions (IO, IV, IOV).

We found no clear desynchronization in the global map analysis under the IA condition. However, we highlighted bilateral desynchronization during IO conditions, centered over the C3 and C4 electrodes, which was completed with bilateral centro-parietal (CP5, CP6) desynchronization. During the IOV condition, we also observed bilateral desynchronization, which was much stronger than that in the other conditions and was mainly centered over the centro-parietal regions and frontal regions. Interestingly, we observed parieto-occipital

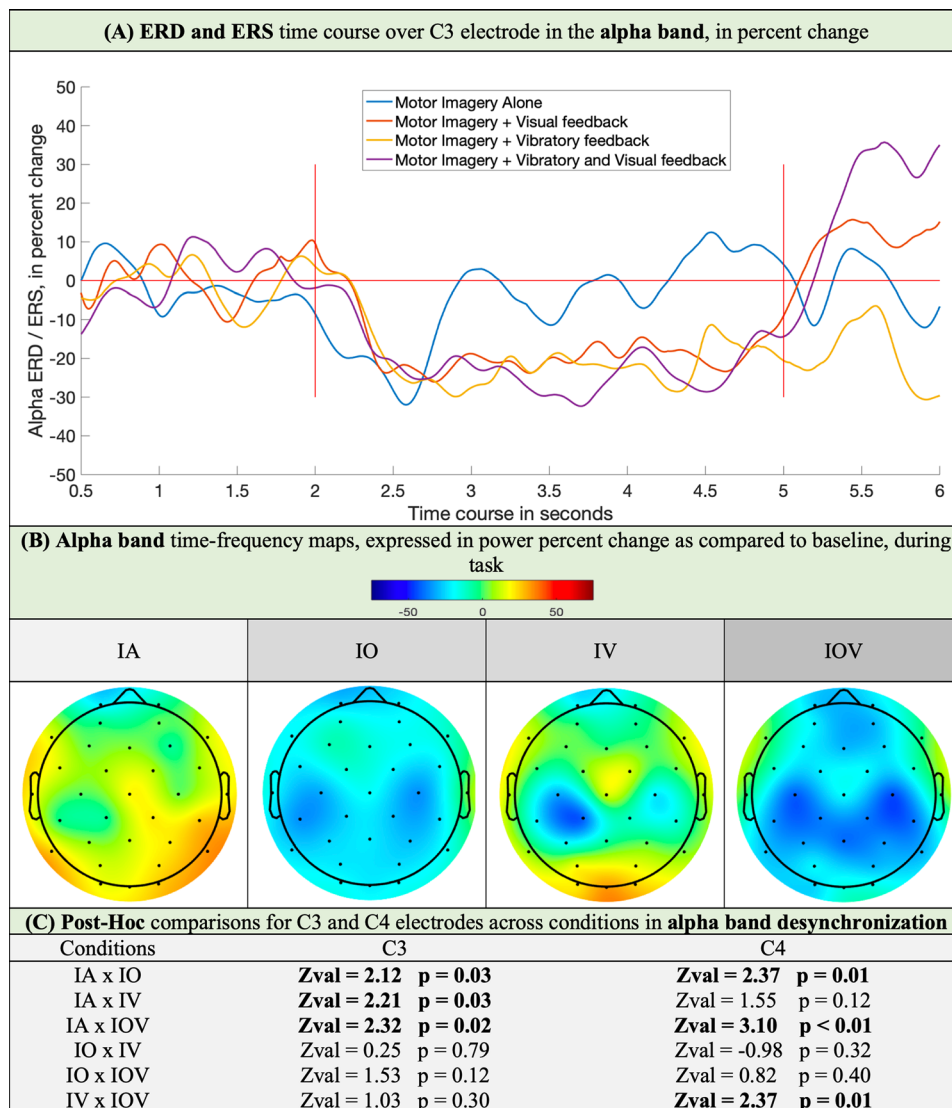


Fig. 4 (A) ERS and ERD time course over the C3 electrode in the alpha band expressed as percent change; the motor imagery task lasted between 2 and 5 s. (B) Time-frequency cortical maps in the alpha band during the motor imagery task with different feedbacks. (C) Statistical analysis of C3 and C4 electrodes between conditions (IA: Motor Imagery Alone, IO: Motor Imagery and Action Observation, IV: Motor Imagery and Focal Vibration, IOV: Motor Imagery and Action Observation and Focal Vibration). For statistical comparison, * indicates significant results

hypersynchrony in the conditions without visual feedback (IA, IV), which was absent in the conditions with visual feedback (IO, IOV) (Fig. 4B).

A statistical comparison of conditions with a Friedman test revealed a significant difference in desynchronization strength across conditions over C3 ($\chi^2(3)=5.4, p=0.021$) and C4 ($\chi^2(3)=8.76, p=0.032$). Post hoc analysis over C3 showed stronger desynchronization over the C3 electrode in the IO, IV and IOV conditions than in the IA condition. Other comparisons over C3 did not show differences between conditions. At the C4 electrode, there was greater desynchronization in the IO and IOV than in the IA and greater desynchronization in the IOV than in the IV (Fig. 4C).

The time-frequency maps of the central (C3, C4), occipital (mean of O1, Oz and O2) and central-parietal (CP5, CP6) regions and the results of the statistical analysis with permutation testing can be found in Tables 1, 2, 3, 4 and 5 of the Supplementary Material.

Beta band desynchronization

In the beta band, the time course analysis of the signal over the C3 electrode showed that in all conditions, desynchronization was maintained throughout the task (Fig. 5A).

In the IA condition, we found weak desynchronization over C3. In the IO condition, there was bilateral desynchronization centered over the C3 and C4 electrodes as

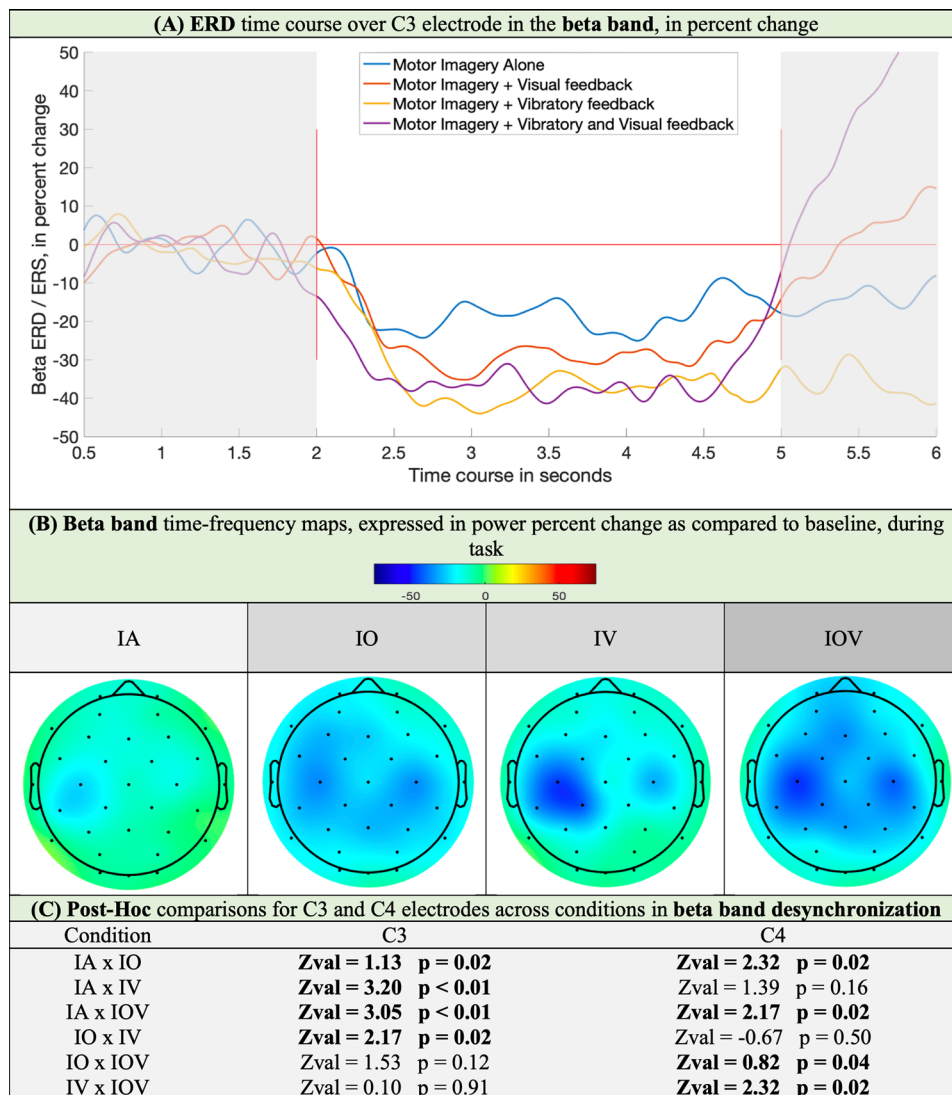


Fig. 5 (A) ERD time course (2 to 5 s) over the C3 electrode in the beta band expressed as percent change; the motor imagery task lasted between 2 and 5 s. (B) Time-frequency cortical maps in the beta band during the motor imagery (MI) task with different feedbacks. (C) Statistical analysis of C3 and C4 electrodes between conditions (IA: motor imagery alone, IO: motor imagery and action observation, IV: motor imagery and focal vibration, IOV: motor imagery and action observation and focal vibration)

well as the left prefrontal and bilateral parietal electrodes. In the IV condition, there was strong left centro-parietal desynchronization, which also involved left precentral electrodes, and weak desynchronization over the right central region (C4). In the IOV condition, the desynchronization was bilateral, much stronger than that in the other conditions, and was mainly centered in bilateral centro-parietal electrodes (CP5, CP6) and left prefrontal electrodes. There were no changes in the occipital electrodes (Fig. 5B).

Statistical comparison of conditions with a Friedman test revealed a significant difference in desynchronization strength across conditions over C3 ($\chi^2 (3) = 13.96$, $p = 0.03$) and C4 ($\chi^2 (3) = 10.36$, $p = 0.015$). Post hoc statistical analysis revealed a significant change in C3 in the

IO, IV, and IOV conditions compared to the IA condition. Desynchronization was also greater in the IV group than in the IO group. At the C4 electrode, desynchronization was greater in the IO and IOV than in the IA. Desynchronization was also greater in the IOV group than in the IV and IO groups (Fig. 5C).

The time-frequency maps of the central (C3, C4) and centro-parietal (CP5, CP6) regions and the results of the statistical analysis with permutation testing can be found in Tables 1, 2, 3, 4 of the Supplementary Material.

Time-frequency analysis after motor imagery

The beta band ERS time course over the C3 electrode can be seen in Fig. 5A between 5 and 6 s.

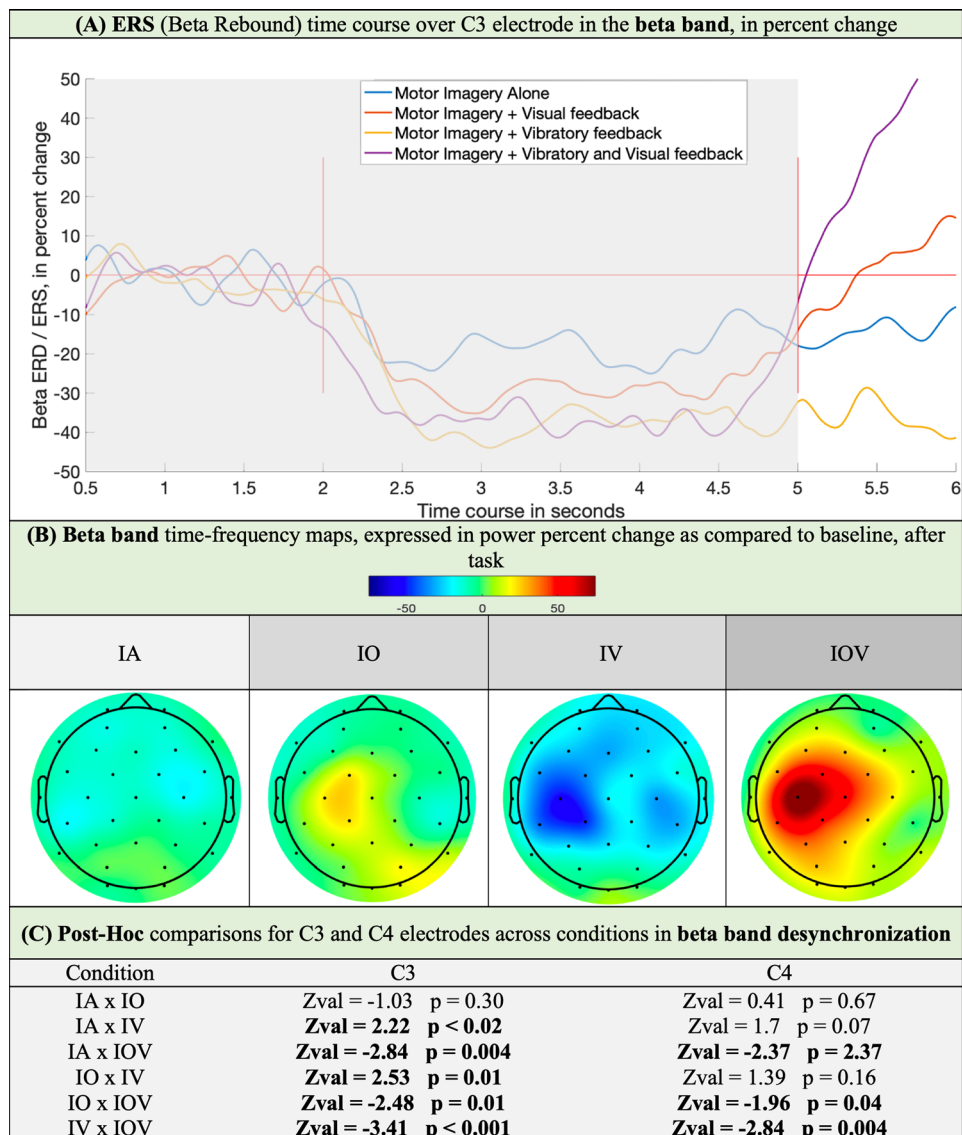


Fig. 6 (A) ERS time course (5 to 6 s) over the C3 electrode in the beta band expressed as percent change; duration of the motor imagery task ranged between 2 and 5 s. (B) Time-frequency cortical maps in the beta band after the motor imagery (MI) task with different feedbacks. (C) Statistical analysis of C3 and C4 electrodes between conditions (IA: motor imagery alone, IO: motor imagery and action observation, IV: motor imagery and focal vibration, IOV: motor imagery and action observation and focal vibration)

After the movement (Fig. 6A, B), there was no ERS (or beta rebound) in the IA condition. With visual feedback (IO, IOV), there was a rebound centered above the C3 electrode, which was stronger in the IOV than in the IO. Under IV conditions, we did not observe any rebound but rather prolonged desynchronization. Analysis of the power time course over C3 showed that in IV, this desynchronization lasts approximately 1 s after the end of the task and then returns to baseline with no rebound. Statistical comparison of conditions with a Friedman test revealed a significant difference in desynchronization strength across conditions over C3 ($\chi^2 (3) = 21.246$, $p < 0.0001$) and C4 ($\chi^2 (3) = 11.72$, $p = 0.008$). Post hoc statistical analysis of C3 (Fig. 6C) revealed significant

differences between all conditions except for the IA × IO comparison. At the C4 electrode, differences were found in the IOV compared to all other conditions.

Motor illusion assessment

Double feedback (IOV) maximized the embodiment in the task (Fig. 7A) and the perceived angle of movement (Fig. 7B). Vibratory feedback also provided a strong kinesthetic illusion (31°, 6/10 illusion intensity), whereas visual feedback alone and motor imagery alone provided weaker embodiment in the task. A statistical comparison of conditions with a Friedman test revealed a significant difference in the perceived intensity of the illusion across the four sensory feedback conditions ($\chi^2 (3) = 21.41$,

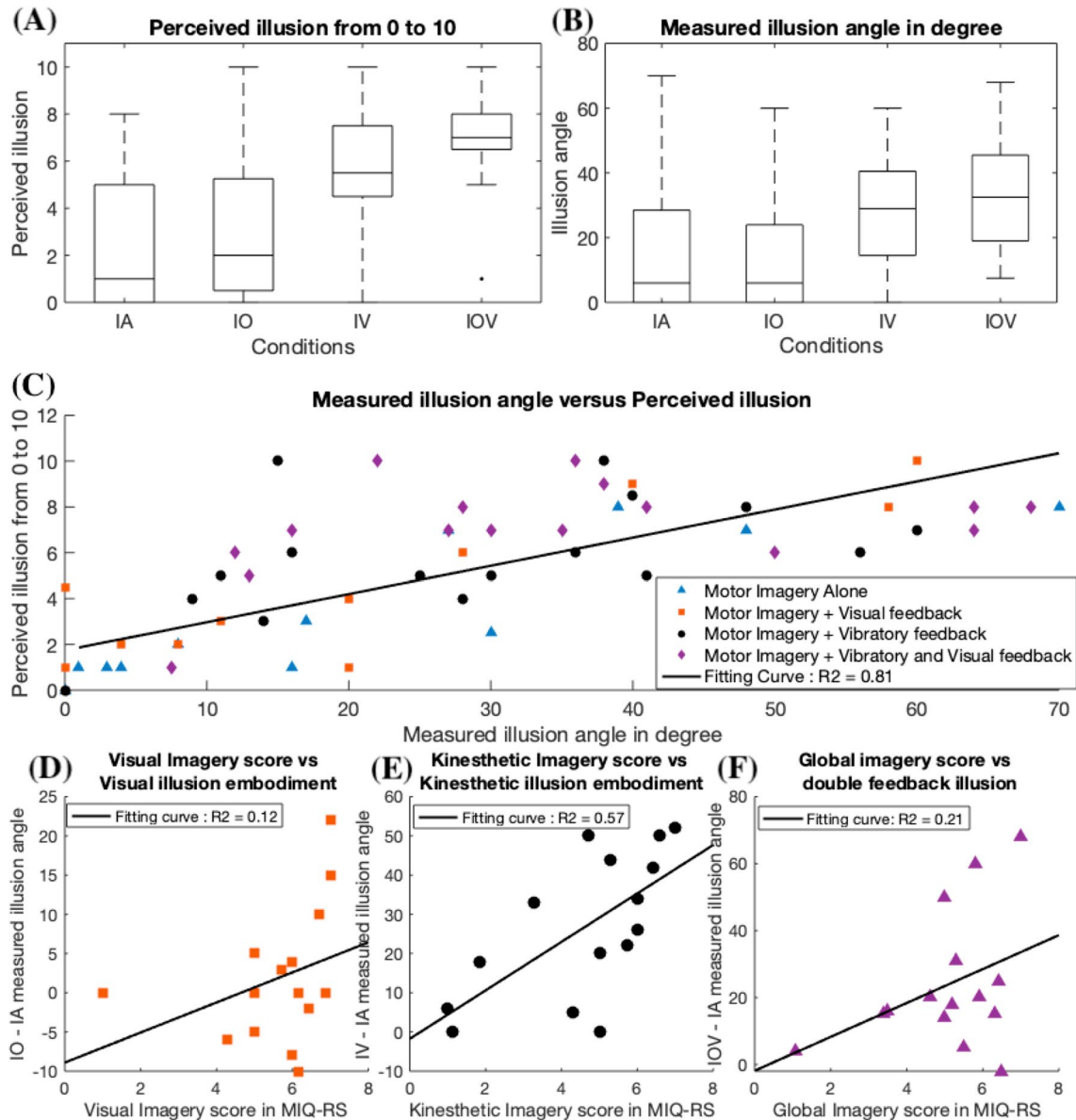


Fig. 7 (A) Mean perceived kinetic illusion amplitude on a Likert scale from 0 (no movement) to 10 (maximum illusion) with standard deviation (red line) in the different conditions. (B) Measured mimicked illusion angle after the task with standard deviation (red line) in the different conditions. (C) Measured illusion angle versus perceived illusion intensity for each condition. (D) Improvement in the illusion angle in the IO condition versus the IA condition (IO angle - IA angle) according to visual imagery performance. (E) Improvement in illusion angle in the IV condition versus the IA condition (IV angle - IA angle) according to kinesthetic imagery performance. (F) Improvement in the illusion angle in the IOV condition versus the IA condition (IOV angle - IA angle) according to global imagery performance (IA: imagery alone, IO: imagery and observation, IV: imagery and vibration, IOV: imagery and observation and vibration)

$p < 0.001$). Subsequent pairwise comparisons using the Wilcoxon signed-rank test indicated that participants perceived a significantly greater illusion intensity in IV compared with IA ($Z = -2.34, p = 0.006$), IOV compared with IA ($Z = -3.2, p = 0.001$), IV compared with IO ($Z = -2.27, p = 0.02$), IOV compared with IO ($Z = -3.04, p = 0.002$) and IOV compared with IV ($Z = -2.47, p = 0.01$). However, we found no significant difference in IO compared with IA ($Z = -1.98, p = 0.04$) (Fig. 7A, B).

We found a good correlation between the subjects' self-declared kinesthetic illusion intensity and the measured angle of their hand mimicking the movement ($R^2 = 0.81$) (Fig. 7C).

We found no significant correlation between the improvement in the illusion angle during IO and the MIQ-RS visual imagery score ($R^2 = 0.12$, Fig. 7D). We found a correlation between embodiment in vibratory therapy and kinesthetic imagery scores on the MIQ-RS

($R^2=0.57$, Fig. 7E). However, we found no significant difference between the improvement in the illusion angle in IOV and the MIQ-RS global imagery score ($R^2=0.21$, Fig. 7F). Compared with neurophysiological data, we did not find any correlation between desynchronization intensity and global motor imagery abilities on the MIQ-RS ($R^2=0.07$) or between desynchronization intensity and perceived motion angle ($R^2=0.009$).

Discussion

The main aim of this study was to highlight brain activation topographic differences among four different conditions of neurofeedback during motor imagery: no feedback, visual feedback, proprioceptive feedback, and combined feedback (visual and proprioceptive).

Visual feedback favors the recruitment of neurons to the visual cortex and mirror system

In the alpha band, we observed strong desynchronization in conditions with visual feedback (IO, IOV) above the bilateral central and parietal regions. In conditions without visual feedback (IA, IV), this desynchronization was much more lateralized in central regions contralateral to the imagined hand movement. In addition, we observed strong parieto-occipital hypersynchrony (increase in alpha activity) in conditions without visual feedback. In contrast, this hypersynchrony was not observed in conditions with visual feedback.

Concerning the modulations of alpha activity in the parieto-occipital regions, we know that these regions support the occipital alpha rhythm, which is well known to electrophysiologists. Indeed, alpha occipital is a brain rhythm. Its power increases when people's eyes are closed, and occipital alpha activity can be used as an index of the degree to which visual brain activity is subjected to inhibition [36]. Occipital alpha activity also reacts to retinotopic amplitude modulation during shifts in visual attention [37], and it is strongly associated with reductions in visual attention [38, 39]. It also acts as a clock on visuo-temporal processing [40]. In sEEG, the occipital alpha rhythm is localized over a large portion of the visual cortex, in the cuneus and calcarine cortex, to a lesser extent in the superior parietal lobule, and in the temporal regions [41]. It originates from the basal ganglia, more specifically in the pulvinar nucleus of the thalamus [42]. Thus, we can reasonably consider that the presence of strong occipital alpha activity in conditions without visual feedback (IA, IV) reflects a relative resting of the occipital cortex and, more specifically, visual areas compared to conditions with visual feedback (IO and IOV) that require visual attention.

The dynamics of alpha desynchronization above central regions correspond to different brain rhythms. Conditions with visual feedback (IO, IOV) are associated

with bilateral centro-parietal alpha desynchronization. Above the sensory-motor regions, alpha band desynchronization is generally associated with Mu desynchronization [43]. The Mu rhythm is a well-known EEG rhythm containing two independent components, one in the alpha band and one in the beta band, encoding different parameters related to motricity [44]. In the alpha band, although it supports a wide range of activities, Mu desynchronization is generally a good marker of the activity of the mirror neuron system (MNS) [45]. This activity is present not only during action observation, motor imagery, and motor execution but also in other more complex tasks recruiting mirror neurons, notably in social cognition [46]. Mu rhythms are generated around bilateral centro-parietal regions [47]. We thus assume that the bilateral alpha desynchronization (absent in IA) we observed corresponds to Mu desynchronization and is proof of the recruitment of the mirror neuron system specific to visual feedback conditions, whereas the lateralized alpha desynchronization in the IV condition is due to another mechanism that we will describe later. This bilateral recruitment has also been observed in other works in healthy subjects [48, 49] and stroke subjects [50]. This hypothesis of MNS recruitment is also supported by the recruitment of the visual cortex in both the IO and IOV conditions (no occipital alpha hypersynchrony), which is a prerequisite for MNS recruitment. This MNS recruitment during visual feedback therapies has already been documented for MT after stroke [1].

Visual feedback enhances motor validation mechanisms

After movement, we observed a stronger beta rebound over the C3 electrode in conditions with visual feedback than in the IA condition. Beta rebound corresponds to hypersynchrony in the beta band following movement [34, 51]. It originates in the motor cortex and can be measured throughout the precentral gyrus [52, 53]. Beta rebound was described as participating in the maintenance of an idling state in sensorimotor regions. However, its interpretation has been broadened: beta rebound is modulated by motor validation phenomena and temporal integration of somatosensory and motor parameters [54] and is related to post-movement motor validation mechanisms. For example, the observation of an erroneous movement modulates beta rebound [55], as can the introduction of errors in a motor task [56]. It is possible that this modulation of beta rebound emerges following the detection of a mismatch between the forward model and the sensory afferents, allowing an update of the motor pattern [57]. The very weak or absent rebound in the IA task may be related to the absence of sensory afference (visual or kinesthetic) to compare with the motor imagery forward model. In contrast, in the IO and IOV conditions, the visual feedback provided to the

subjects, with the precise parameters of the movement, allows this forward model versus sensory afferential comparison, leading to the emergence of a beta rebound. Interestingly, the double feedback condition, which also leads to the strongest embodiment, leads to stronger beta rebound.

Concerning beta rebounds, another point of interest is the absence of beta rebound in the IV condition and the pursuit of desynchronization for approximately 1 s before returning to baseline. Proprioceptive feedback has also been shown to modulate beta rebound, as abolition of proprioceptive feedback leads to a suppression of beta rebound [58]. The presence of beta rebound has been documented after tendinous focal vibration [59], but it is not clear whether, in this experimental paradigm, the subject was allowed to watch his arm during the illusion. In our study, this delay in desynchronization may have been caused by inertia when the vibration device was stopped. However, this hypothesis does not seem valid because the vibration is stopped at the end of the wrist extension phase (at 4 s). Moreover, in the IOV condition, the rebound appears at the end of the movement. Furthermore, even after the return to baseline, between 6 and 7 s, we observed no beta rebound in the IV condition. It is possible that long desynchronization is related to a remanent effect of vibration on sensory-motor regions due to the intensity of vibratory feedback and incongruent signals of neuromuscular bundles that cannot be evened by visual observation. Another hypothesis would be that vibratory feedback alone is insufficient to trigger beta rebound in the absence of visual feedback during motor imagery; indeed, vibration offers a single, continuous sensory afference modality on a single tendon, which is hardly congruent with the actual feeling of a subject who breaks down all the phases of a movement with his hand involving numerous muscles and different movements. One method of testing this hypothesis would be to evaluate beta rebound modulations in two tendon vibration situations: one where the subjects can see their vibrated hand and one where the hand is invisible. We believe that the rebound would be present but weak in the situation where the hand is visible, but this hypothesis remains to be demonstrated.

Vibratory feedback enhances sensorimotor cortex recruitment

When assessing the correlation between the EEG signal intensity of the IV and differences between the IA and IO conditions during the task, we found that there was strong and very lateralized left central (C3) and left centro-parietal (CP1, CP5) desynchronization in both the alpha and beta bands in the IV condition. Having no visual feedback in the IV condition and a different and very lateralized ERD topography, we cannot interpret this

desynchronization as the recruitment of the MNS system, as we observed in IO and IOV. Previous work also demonstrated that when combining MT to FV, stronger alpha desynchronization over C3 occurred under vibration conditions [21]. In fact, in the alpha band, this very lateralized desynchronization in IV during upper limb FV has also been observed in acute stroke patients with an enhancement of alpha ERD (but not beta) over the C3 electrode during right limb FV, suggesting a specific effect of vibration on contralateral S1–M1 excitability [60]. For healthy subjects, vibrotactile vibration is also significantly associated with vibration intensity in the alpha band [61]. For the IV condition, we thus hypothesize that the strong and lateralized desynchronization in the alpha band we observed could be due to specific recruitment of the contralateral sensorimotor cortex due to the right wrist FV.

In the beta band, IV desynchronization is also very lateralized. Beta ERD corresponds to disinhibition of somatomotor neuronal populations [44], with a correlation between motor response intensity and desynchronization strength in stroke patient populations [62]. Beta ERD is also correlated with M1 excitability [63]. For upper limb movements, beta ERD is classically mainly localized on the sensorimotor cortex opposite to the moving limb [64]. These data suggest that the beta band ERD observed in our study during IV conditions reflects strong, specific, and lateralized recruitment of the sensorimotor cortex and primary motor cortex induced by FV therapy. This strong C3 beta ERD is also present in the IOV condition (but more lateralized probably due to the addition of visual feedback effects), which is still consistent with this interpretation.

Kinesthetic feedback is a prerequisite for strong motor illusions in healthy subjects

When assessing motor illusion, it appears that subjects feel more embodiment (declared illusion and measured illusion angle) in conditions with vibratory feedback (IV, IOV) compared with conditions without vibratory feedback (IA, IO), with a good correlation between self-declared illusion and measured illusion angle, increasing the reliability of the data. We found a relatively good correlation ($R^2 = 0.58$) between the kinesthetic motor imagery score on the MIQ-RS and the measured illusion angle in the IV condition. However, we found no such correlation between the visual imagery score on the MIQ-RS and the measured illusion angle in the IO condition ($R^2 = 0.12$) or between the global imagery score on the MIQ-RS and the measured illusion angle in the double feedback condition ($R^2 = 0.21$).

The sense of limb position depends on a convergence of visual and proprioceptive cues [65], and both occipital and somatosensory cortices are involved in the

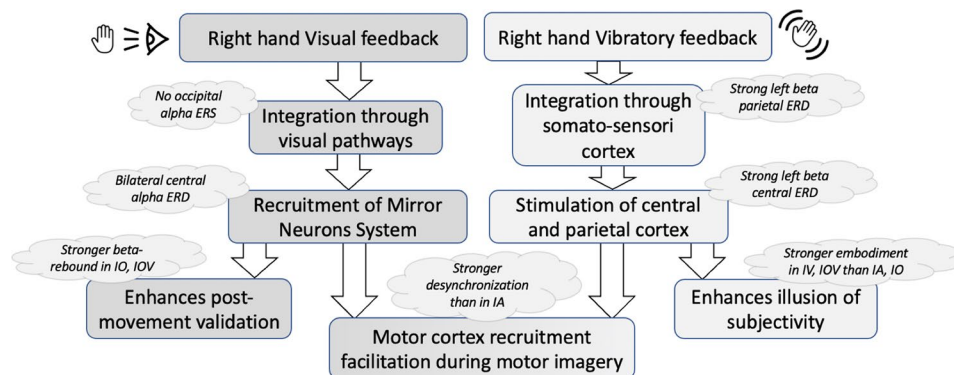


Fig. 8 Global model for visual and vibratory feedback with cortical recruitment consequences and neurophysiological correlates

constitution of feelings of body ownership and the sense of agency in relation to multisensory regions (fronto-parietal cortex), the precuneus and the insular cortex [66]. Our result may seem unexpected because we would have thought that subjects with stronger visual imagery scores would feel more embodiment in the visual feedback condition and that subjects with kinesthetic imagery scores would feel more embodiment in the vibratory feedback condition.

We explain this difference by the presence of a visual-proprioceptive mismatch in the visual feedback (IO) condition, which could diminish the embodiment of the subjects in the task. Indeed, in the IV condition, the subject's hand is masked; thus, he relies exclusively on proprioceptive feedback to build a sense of agency. This finding explains the good correlation between kinesthetic motor imagery performance and the measured illusion angle. In contrast, in the IO condition, the subject can see the hand's movement on the screen but also receives proprioceptive feedback from his or her nonmoving hand, thus creating a visuo-proprioceptive mismatch that reduces embodiment. Adding vibratory feedback to the IO condition (IOV) corrects this visuo-proprioceptive mismatch and thus provides maximal embodiment during therapy.

We did not find any significant correlation between global motor imagery performance on the MIQ-RS and illusion performance in the IOV condition. Furthermore, the addition of the two feedbacks in the IOV condition did not lead to the maximum illusion effect for all the subjects. This may be due to qualitative aspects of the feedback, which may not perfectly reproduce the imagined movement but possibly to the imaging task needed. Subjects may also have different strategies to interpret both proprioceptive and visual feedback. Some subjects reported that they were helped by the feedback, whereas others reported that they were disturbed by it during their motor imagery. Notably, these points remain to be explored through the study of incongruent proprioceptive feedback.

Building a global understanding model

Based on the literature and the results of this research, we propose a general theoretical model for the integration of visual and vibratory feedback in healthy subjects (Fig. 8).

In video feedback therapy, visual feedback is integrated into the occipital cortex and visual areas (no alpha hypersynchrony). This visual feedback of subjective movement recruits mirror neurons (bilateral alpha desynchronization), the involvement of which has been described in visual feedback therapies (MT, virtual reality therapy, etc.) [67–69]. This recruitment of mirror neurons by action observation is also accompanied by the recruitment of sensory-motor regions [67], with an increase in the excitability of the M1 cortex [70–72], connectivity changes [73], and a shift in the interhemispheric balance in healthy subjects and patients in MT [16, 17]. Interestingly, this modulation of M1 by the MNS has been demonstrated in other situations, such as disturbed versus undisturbed movements [74], also suggesting this relationship between the MNS involved in the direct matching model mechanism during action observation [68] and M1 recruitment [75]. This visual feedback also enables the subject to concentrate and work on the fine parameters of movement, which results in a greater beta rebound than during motor imagery alone because the subject is provided with feedback on the movement. Beta rebound relations with the mirror neuron system and Mu rhythms have been explored in autism [76], but we have few points of comparison for healthy subjects or neurological patients. A pitfall of visual feedback therapy alone is that the visual illusion seems to conflict, at least for some subjects, with the proprioceptive feedback of the immobile limb, which diminishes the movement illusion at the group level.

In FV therapy, feedback integration is mediated by a different pathway involving somatosensory cortex recruitment (alpha desynchronization) [60], leading to global recruitment of sensory-motor regions (beta desynchronization) in healthy subjects [77] and stroke

patients [78]. This recruitment may also be accompanied by modulation of corticospinal excitability, although this point is still discussed in the literature [18, 79, 80]; corticospinal plasticity [81]; connectivity changes and improvement of efficiency parameters in stroke patients [19, 20]; and remnant and additive effects of M1 excitability immediately following the end of vibrations [60]. This recruitment also favors the emergence of a strong kinesthetic illusion, at least in situations where visual feedback is hidden, with a good correlation between the subjects' kinesthetic imagery abilities and their sensation of embodiment. However, vibration of a single tendon does not provide the subject with a precise model of the movement on which to base his motor imagery (on/off vibration of a single tendon) and may therefore not favor the emergence of beta rebound and postmovement validation mechanisms. However, further studies are needed to study beta rebound after vibration therapy.

In the double feedback condition, these two pathways are solicited concomitantly (strong bilateral desynchronization, but that also seems reinforced over the left central regions) with probable potentiation because we observe a statistically significantly reinforced rebound (visual pathway) along with a strong sensation of embodiment (vibratory pathway). A stronger sense of embodiment has also been documented when combining MT and vibrotactile stimulation [82, 83], leading to strong M1 excitability [84], which is a function of the vividness of the kinesthetic illusion perceived by the subjects [85]. Congruent visuo-proprioceptive feedback induces strong M1 excitability, whereas simple tactical stimulation coupled with action observation alone does not. This study focused on healthy subjects. However, in our view, these data suggest that during neurological rehabilitation (stroke, brachial plexus palsy, etc.), the types of feedback should be adapted for each subject while remaining as varied as possible for stimulating both integration pathways.

From healthy subjects to neurological patients

Since this study was conducted on healthy subjects, we must exercise caution when applying these results to a pathological population, as they may have significantly different brain rhythms and functional cortical dynamics [86]. However, some general conclusions can be drawn.

Firstly, this study confirms that both visual and proprioceptive feedback enhance the recruitment of the sensorimotor cortex compared to motor imagery tasks alone. This effect is even more pronounced in the double feedback condition. Based on these results, which demonstrate stronger cortical recruitment in the double feedback condition, as well as findings from the literature showing better functional outcomes with double

feedback [87], we recommend providing patients with combined feedback whenever possible.

Another point of interest is the presence of different feedback integration networks, which are based on distinct anatomical structures. Although the exact mechanisms by which visual and proprioceptive feedback recruit the motor cortex are still debated, we can speculate that specific lesions in these pathways may impair feedback integration in pathological subjects. For instance, the modulation of cortical recruitment varies according to lesion topography in focal vibration [88], with a stronger recruitment observed in patients with basal ganglia ischemia and other subcortical ischemia, compared to those with cortical strokes. There are few comparable studies in the literature for visual feedback therapies. In a context where patients often engage with various rehabilitation devices indiscriminately, determining which type of feedback most effectively promotes motor cortex recruitment for each patient may be crucial for personalizing therapies [26].

Limitations

The main limitation of this study lies in the small number of subjects included. Although statistically significant results were obtained in the areas of interest, these findings need to be validated in a larger sample. Furthermore, this study included only right-handed subjects. It would be interesting to investigate the effect of feedback laterality on handedness in a larger cohort (e.g., left-hand motor imagery and feedback for right-handed subjects). Finally, it will be necessary to test these results with other rehabilitation methods (such as virtual reality, robotic therapy, etc.), both in healthy subjects and patients, to confirm the validity of this model.

Additionally, we did not include a sham condition for the vibration to distinguish between the specific recruitment of the sensorimotor cortex caused by tendinous vibration and the recruitment induced by the sensation of the vibratory device's movements. Indeed, both proprioceptive and sensory feedback have correlates in the alpha and beta bands [89], which can be confounded in the analysis. Given the strong motor illusion reported by the subjects, we believe the cortical effects were primarily due to the proprioceptive aspect of the feedback. However, further research should investigate this point and include a vibratory sham condition.

Finally, a longer time at the beginning of the epochs should also be considered. Indeed, our baseline may also have been contaminated by some motor-preparation rhythms. Statistical comparison was performed between time-frequency maps with different baselines (500–1500ms baseline versus 500–1200ms baseline) and found no difference. Even if this did not change the overall significance of our results, further studies should include

at least three seconds of pause at the beginning of each epoch.

Conclusion

This study compared differences in cortical activation around sensory-motor regions during a motor imagery task with different neurofeedback modalities: no feedback, visual feedback, tendon vibration feedback, and visual and vibratory feedback.

We found differences in cortical recruitment, indicating different modalities of integration of visual and proprioceptive feedback. Visual feedback leads to the recruitment of the MNS, favors motor validation mechanisms, and recruits sensorimotor areas but does not provide a strong movement illusion. Vibratory feedbacks recruit sensorimotor areas and enhances the illusion of movement but does not specifically favor motor validation. Double feedback combines the effects of both techniques, strongly recruits the sensorimotor cortex with a potentiation effect and maximizes post-movement validation and the feeling of embodiment.

In this work, we propose a specific model for studying the visual and proprioceptive afferents involved in all motor rehabilitation techniques. Our next step is to study this model on a larger set of healthy subjects and in a pathological situation (i.e., stroke) to evaluate how these afferences are integrated on the assumption that, in a pathological situation, certain patients would be more receptive to one type of feedback than another.

Abbreviations

| | |
|------|---|
| EEG | Electroencephalography |
| ERD | Event Related Desynchronization |
| ERS | Event Related Synchronization |
| fMRI | Functional Magnetic Resonance Imagery |
| FV | Focal Vibration |
| FWHM | Full Width at Half Maximum |
| MI | Mental Imagery |
| MNS | Mirror Neuron System |
| IA | Mental Imagery Alone condition |
| IO | Mental Imagery + Action Observation condition |
| IOV | Mental Imagery + Action Observation + Focal Vibration condition |
| IV | Mental Imagery + Focal Vibration condition |
| MNS | Mirror Neurons System |
| MT | Mirror Therapy |
| VFT | Visual Feedback Therapies |
| VOT | Video Observational Therapy |
| VR | Virtual Reality |

Supplementary Information

The online version contains supplementary material available at <https://doi.org/10.1186/s12984-024-01453-3>.

- Supplementary Material 1
- Supplementary Material 2
- Supplementary Material 3
- Supplementary Material 4
- Supplementary Material 5

Acknowledgements

The EEG device and disposable were funded by the Association AIRE (St-Etienne, France) and by the Foundation Neurodis (St-Etienne, France). The funders had no role in the study design, data collection and analysis, decision to publish or preparation of the manuscript. This article was edited for proper English language at AJE: EB03-07F6-62DD-8C91-4298.

Author contributions

AA and RD performed the experiments. AA analyzed the data, with help of SL. AA wrote the paper with BH and OE. AA, RD and GP conceived the study. GP supervised the study. All the authors contributed to the editing of this paper.

Funding

The EEG device and disposable were funded by the *Association AIRE* (St-Etienne, France) and by the *Foundation Neurodis* (St-Etienne, France). The funders had no role in the study design, data collection and analysis, decision to publish or preparation of the manuscript.

Data availability

The datasets supporting the conclusions of this article are available upon reasonable request.

Declarations

Ethical approval

The study OPTIVBE was registered and approved by the ethics committee CPP: "Comité de protection des personnes Sud Ouest et Outre Mer IV" (04/12/2019. N°: CPP2019-11-084a / 2019-A01673-54 / 19.09.12.44858 with amendment N°: 19.01592.201984-MS03 allowing EEG data collection for healthy subjects). The study was conducted in accordance with the Declaration of Helsinki.

Human ethics and consent to participate

Written consent was obtained from all the subjects for participation and publication.

Competing interests

The authors declare no competing interests.

Author details

¹Department of Physical Rehabilitation, CHU of St Etienne, St-Etienne, France

²Laboratory Trajectoires, INSERM 1028, CNRS 5229, University of Lyon-St-Etienne, St-Etienne, France

³Inter-University Laboratory of Human Movement Biology, "Physical Ability and Fatigue in Health and Disease" Team, Saint-Etienne "Jean Monnet" & Lyon 1 & "Savoie Mont- Blanc" Universities, Saint- Etienne F-42023, France

⁴Univ. Grenoble Alpes, CEA, LETI, Clinatec, Grenoble, France

Received: 7 April 2024 / Accepted: 20 August 2024

Published online: 12 September 2024

References

1. Villa-Berges E, Laborda Soriano AA, Lucha-López O, Tricas-Moreno JM, Hernández-Securún M, Gómez-Martínez M, et al. Motor Imagery and Mental Practice in the Subacute and Chronic Phases in Upper Limb Rehabilitation after Stroke: a systematic review. Costi S, éditeur. Occup Therapy Int 24 janv. 2023;2023:1-12.
2. Filgueiras A, Quintas Conde EF, Hall CR. The neural basis of kinesthetic and visual imagery in sports: an ALE meta-analysis. Brain Imaging Behav Oct. 2018;12(5):1513–23.
3. Hétu S, Grégoire M, Saimpont A, Coll MP, Eugène F, Michon PE, et al. The neural network of motor imagery: an ALE meta-analysis. Neurosci Biobehavioral Reviews juin. 2013;37(5):930–49.
4. Monteiro KB, Cardoso M, dos S, Cabral VR da, Santos C, dos AOB, Silva PS da, de Castro JBP et al. Effects of Motor Imagery as a Complementary Resource on the Rehabilitation of Stroke Patients: A Meta-Analysis of Randomized Trials. Journal of Stroke and Cerebrovascular Diseases. août. 2021;30(8):105876.

5. Machado TC, Carregosa AA, Santos MS, Ribeiro NM, da Melo S. Efficacy of motor imagery additional to motor-based therapy in the recovery of motor function of the upper limb in post-stroke individuals: a systematic review. *Top Stroke Rehabil.* oct 2019;3(7):548–53.
6. Bajaj S, Butler AJ, Drake D, Dhamala M. Brain effective connectivity during motor-imagery and execution following stroke and rehabilitation. *NeuroImage: Clin.* 2015;8:572–82.
7. Cicinelli P, Marconi B, Zaccagnini M, Pasqualetti P, Filippi MM, Rossini PM. Imagery-induced cortical excitability changes in stroke: a transcranial magnetic stimulation study. *Cereb Cortex* 1 févr. 2006;16(2):247–53.
8. Tavazzi E, Bergsland N, Pirastu A, Cazzoli M, Blasi V, Baglio F. MRI markers of functional connectivity and tissue microstructure in stroke-related motor rehabilitation: a systematic review. *NeuroImage: Clin.* 2022;33:102931.
9. Kim H, Lee E, Jung J, Lee S. Utilization of Mirror Visual Feedback for Upper Limb function in Poststroke patients: a systematic review and Meta-analysis. *Vis 15 nov.* 2023;7(4):75.
10. Altschuler EL, Wisdom SB, Stone L, Foster C, Galasko D, Llewellyn DME, et al. Rehabilitation of hemiparesis after stroke with a mirror. *Lancet* juin. 1999;353(9169):2035–6.
11. Ding L, Wang X, Chen S, Wang H, Tian J, Rong J, et al. Camera-based Mirror Visual Input for Priming Promotes Motor Recovery, daily function, and Brain Network Segregation in Subacute Stroke patients. *Neurorehabilitation Neural Repair* avr. 2019;33(4):307–18.
12. Borges LR, Fernandes AB, Melo LP, Guerra RO, Campos TF. Action observation for upper limb rehabilitation after stroke. *Cochrane Database Syst Rev.* 2018;10(10).
13. Giroux P, Sirigu A. Illusory movements of the paralyzed limb restore motor cortex activity. *NeuroImage* Nov. 2003;20:S107–11.
14. Moggio L, de Sire A, Marotta N, Demeco A, Ammendolia A. Vibration therapy role in neurological diseases rehabilitation: an umbrella review of systematic reviews. *Disabil Rehabil.* sept 2022;25(20):5741–9.
15. Alashram AR, Padua E, Romagnoli C, Annino G. Effectiveness of focal muscle vibration on hemiplegic upper extremity spasticity in individuals with stroke: a systematic review. *NeuroRehabilitation* 18 déc. 2019;45(4):471–81.
16. Bartrum G, Pratt H, Dickstein R, Frenkel-Toledo S, Geva A, Soroker N. Electrophysiological manifestations of mirror visual feedback during manual movement. *Brain Res mai.* 2015;1606:113–24.
17. Bartrum G, Pratt H, Frenkel-Toledo S, Soroker N. Neurophysiological effects of mirror visual feedback in stroke patients with unilateral hemispheric damage. *Brain Res déc.* 2018;1700:170–80.
18. Sourour R, Baudry S, Millet GY, Lapole T. Vibration-induced depression in spinal loop excitability revisited. *J Physiol nov.* 2019;597(21):5179–93.
19. Li W, Li C, Xu Q, Ji L. Effects of Focal Vibration over Upper Limb Muscles on the activation of Sensorimotor Cortex Network: an EEG study. *J Healthc Eng.* 2019;2019:9167028.
20. Li W, Li C, Xiang Y, Ji L, Hu H, Liu Y. Study of the activation in sensorimotor cortex and topological properties of functional brain network following focal vibration on healthy subjects and subacute stroke patients: an EEG study. *Brain Res nov.* 2019;1722:146338.
21. Ding L, He J, Yao L, Zhuang J, Chen S, Wang H, et al. Mirror Visual Feedback combining Vibrotactile Stimulation promotes Embodiment Perception: an Electroencephalogram (EEG) pilot study. *Front Bioeng Biotechnol.* oct 2020;26:8:553270.
22. Le Franc S, Bonan I, Fleury M, Butet S, Barillot C, Lécyuer A, et al. Visual feedback improves movement illusions induced by tendon vibration after chronic stroke. *J Neuro-Engineering Rehabilitation* déc. 2021;18(1):156.
23. Le Franc S, Fleury M, Jeunet C, Butet S, Barillot C, Bonan I, et al. Influence of the visuo-proprioceptive illusion of movement and motor imagery of the wrist on EEG cortical excitability among healthy participants. *Aspell JE, éditeur. PLoS ONE* 2 sept. 2021;16(9):e0256723.
24. Vidaurre C, Ramos Murgulday A, Haufe S, Gómez M, Müller KR, Nikulin VV. Enhancing sensorimotor BCI performance with assistive afferent activity: an online evaluation. *NeuroImage* 1 oct. 2019;199:375–86.
25. Zhang L, Chen L, Wang Z, Zhang X, Liu X, Ming D. Enhancing visual-guided motor imagery performance via sensory threshold Somatosensory Electrical Stimulation Training. *IEEE Trans Biomedical Eng* févr. 2023;70(2):756–65.
26. Le Franc S, Herrera Altamira G, Guillen M, Butet S, Fleck S, Lécyuer A, et al. Toward an adapted Neurofeedback for Post-stroke Motor Rehabilitation: state of the art and perspectives. *Front Hum Neurosci* 14 Juill. 2022;16:917909.
27. Lorant J, Nicolas A. Validation de la traduction française Du Movement Imagery Questionnaire-revised (MIQ-R). *Sci Motricité.* 2004;53:57–68.
28. Mathôt S, Schreij D, Theeuwes J, OpenSesame. An open-source, graphical experiment builder for the social sciences. *Behav Res Methods* juin. 2012;44(2):314–24.
29. Avvantaggiato C, Casale R, Cinone N, Facciorusso S, Turitto A, Stuppiello L, Picelli A, Ranieri M, Intiso D, Fiore P, Ciritella C, Santamato A. Localized muscle vibration in the treatment of motor impairment and spasticity in post-stroke patients: a systematic review. *Eur J Phys Rehabil Med.* 2021;57(1):44–60.
30. Delorme A, Makeig S. EEGLAB: an open source toolbox for analysis of single-trial EEG dynamics including independent component analysis. *J Neurosci Methods* mars. 2004;134(1):9–21.
31. Dong L, Li F, Liu Q, Wen X, Lai Y, Xu P, et al. MATLAB Toolboxes for Reference Electrode standardization technique (REST) of scalp EEG. *Front NeuroSci.* oct 2017;30:11:601.
32. Cohen MX. A better way to define and describe Morlet wavelets for time-frequency analysis. *NeuroImage Oct.* 2019;199:81–6.
33. Allen DP, MacKinnon CD. Time-frequency analysis of movement-related spectral power in EEG during repetitive movements: a comparison of methods. *J Neurosci Methods* janv. 2010;186(1):107–15.
34. Pfurtscheller G, Lopes da Silva FH. Event-related EEG/MEG synchronization and desynchronization: basic principles. *Clin Neurophysiol Nov.* 1999;110(11):1842–57.
35. Maris E, Oostenveld R. Nonparametric statistical testing of EEG- and MEG-data. *J Neurosci Methods* août. 2007;164(1):177–90.
36. Hohalik W, Saurels BW, Johnston A, Yarrow K, Arnold DH. Occipital alpha-band brain waves when the eyes are closed are shaped by ongoing visual processes. *Sci Rep déc.* 2022;12(1):1194.
37. Seward TV, Seward MA. Alpha-band oscillations in visual cortex: part of the neural correlate of visual awareness? *Int J Psychophysiol* 1 avr. 1999;32(1):35–45.
38. Peylo C, Hilla Y, Sauseng P. Cause or consequence? Alpha oscillations in visuospatial attention. *Trends Neurosciences Sept.* 2021;44(9):705–13.
39. Sauseng P, Klimesch W, Stadler W, Schabus M, Doppelmayr M, Hanslmayr S, et al. A shift of visual spatial attention is selectively associated with human EEG alpha activity. *Eur J Neurosci déc.* 2005;22(11):2917–26.
40. Freschl J, Azizi LA, Balboa L, Kaldy Z, Blaser E. The development of peak alpha frequency from infancy to adolescence and its role in visual temporal processing: a meta-analysis. *Dev Cogn Neurosci oct.* 2022;57:101146.
41. Frauscher B, Von Ellenrieder N, Zelmann R, Doležálová I, Minotti L, Olivier A, et al. Atlas of the normal intracranial electroencephalogram: neurophysiological awake activity in different cortical areas. *Brain* 1 avr. 2018;141(4):1130–44.
42. Attal Y, Schwartz D. Assessment of Subcortical Source Localization Using Deep Brain Activity Imaging Model with Minimum Norm Operators: A MEG Study. Barnes GR, éditeur. PLoS ONE. 20 mars. 2013;8(3):e59856.
43. Debnath R, Salo VC, Buzzell GA, Yoo KH, Fox NA. Mu rhythm desynchronization is specific to action execution and observation: evidence from time-frequency and connectivity analysis. *NeuroImage* janv. 2019;184:496–507.
44. Stolk A, Brinkman L, Vansteensel MJ, Aarnoutse E, Leijten FS, Dijkerman CH et al. Electrocorticographic dissociation of alpha and beta rhythmic activity in the human sensorimotor system. *eLife* 9 oct 2019;8:e48065.
45. Fox NA, Bakermans-Kranenburg MJ, Yoo KH, Bowman LC, Cannon EN, Vanderwert RE, et al. Assessing human mirror activity with EEG mu rhythm: a meta-analysis. *Psychol Bull.* 2016;142(3):291–313.
46. Hobson HM, Bishop DVM. The interpretation of mu suppression as an index of mirror neuron activity: past, present and future. *Royal Soc Open Sci* mars. 2017;4(3):160662.
47. Thorpe SG, Cannon EN, Fox NA. Spectral and source structural development of mu and alpha rhythms from infancy through adulthood. *Clin Neurophysiol* Janv. 2016;127(1):254–69.
48. Cole EJ, Barracough NE. Timing of mirror system activation when inferring the intentions of others. *Brain Res* 1 déc. 2018;1700:109–17.
49. Caspers S, Zilles K, Laird AR, Eickhoff SB. ALE meta-analysis of action observation and imitation in the human brain. *NeuroImage* 15 avr. 2010;50(3):1148–67.
50. Franceschini M, Ottaviani M, Romano P, Goffredo M, Pournajaf S, Lofrumento M et al. sept. The reaching phase of feeding and self-care actions optimizes Action Observation effects in chronic stroke subjects. *Neurorehabilitation and neural repair.* 1 2022;36(9):574–86.
51. Pfurtscheller G, Neuper C, Brunner C, Da Silva FL. Beta rebound after different types of motor imagery in man. *Neurosci Lett* Avr. 2005;378(3):156–9.
52. Jurkiewicz MT, Gaetz WC, Boston AC, Cheyne D. Post-movement beta rebound is generated in motor cortex: evidence from neuromagnetic recordings. *NeuroImage* Sept. 2006;32(3):1281–9.

53. Mary A, Bourguignon M, Wens V, Op De Beeck M, Leproult R, De Tiège X, et al. Aging reduces experience-induced sensorimotor plasticity. A magnetoencephalographic study. *NeuroImage* janv. 2015;104:59–68.
54. Cardellicchio P, Hilt PM, Dolfini E, Fadiga L, D'Ausilio A. Beta rebound as an index of temporal integration of Somatosensory and Motor signals. *Front Syst Neurosci* 2 sept. 2020;14:63.
55. Koelewijn T, Van Schie HT, Bekkering H, Oostenveld R, Jensen O. Motor-cortical beta oscillations are modulated by correctness of observed action. *NeuroImage Avr.* 2008;40(2):767–75.
56. Torrecillas F, Alayrangues J, Kilavik BE, Malfait N. Distinct modulations in Sensorimotor Postmovement and Foreperiod β-Band activities related to Error Salience Processing and Sensorimotor Adaptation. *J Neurosci* 16 sept. 2015;35(37):12753–65.
57. Cao L, Hu YM. Beta rebound in Visuomotor Adaptation: still the Status Quo? *J Neurosci* 15 juin. 2016;36(24):6365–7.
58. Cassim F, Monaca C, Szurhaj W, Bourriez JL, Defebvre L, Derambure P, Guieu JD. Does post-movement beta synchronization reflect an idling motor cortex? *NeuroReport*. 2001;12(17):3859–63.
59. Keinrath C, Wriessnegger S, Müller-Putz GR, Pfurtscheller G. Post-movement beta synchronization after kinesthetic illusion, active and passive movements. *Int J Psychophysiol* nov. 2006;62(2):321–7.
60. Lopez S, Bini F, Del Percio C, Marozzi F, Celletti C, Suppa A, et al. Electroencephalographic sensorimotor rhythms are modulated in the acute phase following focal vibration in healthy subjects. *Neurosci* 3 juin. 2017;352:236–48.
61. Park W, Kim SP, Eid M. Neural coding of vibration intensity. *Front Neurosci* 11 Nov. 2021;15:682113.
62. Shiner CT, Tang H, Johnson BW, McNulty PA. Cortical beta oscillations and motor thresholds differ across the spectrum of post-stroke motor impairment, a preliminary MEG and TMS study. *Brain Res déc.* 2015;1629:26–37.
63. Takemi M, Masakado Y, Liu M, Ushiba J. Event-related desynchronization reflects downregulation of intracortical inhibition in human primary motor cortex. *J Neurophysiol* sept. 2013;110(5):1158–66.
64. Zhao M, Marino M, Samogin J, Swinnen SP, Mantini D. Hand, foot and lip representations in primary sensorimotor cortex: a high-density electroencephalography study. *Sci Rep* 19 déc. 2019;9(1):19464.
65. Graziano MSA. Where is my arm? The relative role of vision and proprioception in the neuronal representation of limb position. *Proceedings of the National Academy of Sciences*. 31 août. 1999;96(18):10418–21.
66. Schneider C, Marquis R, Jöhr J, Lopes da Silva M, Ryvlin P, Serino A, De Lucia M, Diserens K. Disentangling the percepts of illusory movement and sensory stimulation during tendon vibration in the EEG. *NeuroImage*. 2021;241:118431.
67. Zhang JJQ, Fong KNK, Welage N, Liu KPY. The activation of the Mirror Neuron System during Action Observation and Action execution with Mirror Visual Feedback in Stroke: a systematic review. *Neural Plast.* 2018;2018:1–14.
68. Kemmerer D. What modulates the Mirror Neuron System during action observation? Multiple factors involving the action, the actor, the observer, the relationship between actor and observer, and the context. *Progress Neurobiol* oct. 2021;205:102128.
69. Brihmat N, Tarri M, Quidé Y, Angllo K, Pavard B, Castel-Lacanal E, et al. Action, observation or imitation of virtual hand movement affect differently regions of the mirror neuron system and the default mode network. *Brain Imaging Behav Oct.* 2018;12(5):1363–78.
70. Lepage JF, Tremblay S, Théoret H. Early non-specific modulation of corticospinal excitability during action observation. *Eur J Neurosci mars.* 2010;31(5):931–7.
71. Strafella AP, Paus T. Modulation of cortical excitability during action observation: a transcranial magnetic stimulation study. *Neuroreport* 14 Juill. 2000;11(10):2289–92.
72. Novaes MM, Palhano-Fontes F, Peres A, Mazzetto-Betti K, Pelicioni M, Andrade KC, et al. Neurofunctional changes after a single mirror therapy intervention in chronic ischemic stroke. *Int J Neurosci oct.* 2018;128(10):966–74.
73. Lin SH, Cheng CH, Wu CY, Liu CT, Chen CL, Hsieh YW. Mirror Visual Feedback Induces M1 Excitability by Disengaging Functional Connections of Perceptuo-Motor-Attentional Processes during Asynchronous Bimanual Movement: A Magnetoencephalographic Study. *Brain Science*. 20 août. 2021;11(8):1092.
74. Cheng CH, Sun HH, Weng JQ, Tseng YJ. Differential motor cortex excitability during observation of normal and abnormal goal-directed movement patterns. *Neurosci Res oct.* 2017;123:36–42.
75. Liepelt R, Cramon DYV, Brass M. What is matched in direct matching? Intention attribution modulates motor priming. *J Experimental Psychology: Hum Percept Perform juin.* 2008;34(3):578–91.
76. Honaga E, Ishii R, Kurimoto R, Canuet L, Ikezawa K, Takahashi H, et al. Post-movement beta rebound abnormality as indicator of mirror neuron system dysfunction in autistic spectrum disorder: an MEG study. *Neurosci Lett* 12 Juill. 2010;478(3):141–5.
77. Ramu V, Lakshminarayanan K. Enhanced motor imagery of digits within the same hand via vibrotactile stimulation. *Front NeuroSci.* 2023;17:1152563.
78. Snyder DB, Beardsley SA, Hyngstrom AS, Schmit BD. Cortical effects of wrist tendon vibration during an arm tracking task in chronic stroke survivors: an EEG study. *PLoS ONE.* 2023;18(12):e0266586.
79. Kolbaşı EN, Huseyinsinoglou BE, Bayraktaroğlu Z. Effect of upper limb focal muscle vibration on cortical activity: a systematic review with a focus on primary motor cortex. *Eur J Neurosci* août. 2022;56(3):4141–53.
80. Lauzier L, Perron MP, Munger L, Bouchard É, Abboud J, Nougarou F, et al. Variation of corticospinal excitability during kinesthetic illusion induced by musculotendinous vibration. *J Neurophysiol* 1 nov. 2023;130(5):1118–25.
81. Rocchi L, Suppa A, Leodori G, Celletti C, Camerota F, Rothwell J, et al. Plasticity Induced in the human spinal cord by focal muscle vibration. *Front Neurol.* 2018;9:935.
82. Ding L, He J, Yao L, Zhuang J, Chen S, Wang H, et al. Mirror Visual Feedback combining Vibrotactile Stimulation promotes Embodiment Perception: an Electroencephalogram (EEG) pilot study. *Front Bioeng Biotechnol.* 2020;8:553270.
83. Schlienger R, De Giovanni C, Guerra M, Kavounoudias A. When proprioceptive feedback enhances visual perception of self-body movement: rehabilitation perspectives. *Front Hum Neurosci* 12 mai. 2023;17:1144033.
84. Bisio A, Biggio M, Canepa P, Faelli E, Ruggeri P, Avanzino L, et al. Primary motor cortex excitability as a marker of plasticity in a stimulation protocol combining action observation and kinesthetic illusion of movement. *Eur J Neurosci avr.* 2021;53(8):2763–73.
85. Bisio A, Biggio M, Avanzino L, Ruggeri P, Bove M. Kinaesthetic illusion shapes the cortical plasticity evoked by action observation. *J Physiol juin.* 2019;597(12):3233–45.
86. Kancheva I, Van Der Salm SMA, Ramsey NF, Vansteensel MJ. Association between lesion location and sensorimotor rhythms in stroke – a systematic review with narrative synthesis. *Neurol Sci déc.* 2023;44(12):4263–89.
87. He J, Li C, Lin J, Shu B, Ye B, Wang J, et al. Proprioceptive training with visual feedback improves Upper Limb function in Stroke patients: a pilot study. *Neural Plast.* 2022;2022:1588090.
88. Li W, Li C, Liu A, Lin PJ, Mo L, Zhao H, et al. Lesion-specific cortical activation following sensory stimulation in patients with subacute stroke. *J Neuroeng Rehabil.* nov 2023;13(1):155.
89. Schneider C, Marquis R, Jöhr J, Lopes da Silva M, Ryvlin P, Serino A, et al. Disentangling the percepts of illusory movement and sensory stimulation during tendon vibration in the EEG. *Neuroimage* 1 nov. 2021;241:118431.

Publisher's note

Springer Nature remains neutral with regard to jurisdictional claims in published maps and institutional affiliations.